Eur Biophys J (2000) 29: 113–124

ARTICLE

W. Meier · G. Greune · A. Meyboom · K.P. Hofmann

Surface tension and viscosity of surfactant from the resonance of an oscillating drop

Received: 22 October 1999 / Revised version: 24 January 2000 / Accepted: 24 January 2000

Abstract The oscillating drop surfactometer (ODS) measures surface tension (γ) and energy dissipation (damping constant b) of surfactant on a 1 µl sample. γ is obtained from the period of oscillation and b from its free decay or from the phase shift slope in resonance. After calibration with substances with different γ, corrections were made for capillary fixation and loss of mass by evaporation. Surface active substances are delivered from liposomes in the interior (subphase) or injected from outside, with microdrops (180 pl each) of solution. As an application example, we have investigated surfactant extract and pure phospholipid. In minutes after formation of a drop containing a diluted Survanta suspension, γ decreases by 20 mN/m, while b increases three-fold. This effect, assigned to spontaneous adsorption from liposomes to the surface, is not seen with pure dipalmitoylphosphatidylcholine (DPPC) under our conditions. However, microdrop injection of DPPC triggers a rapid decrease of γ and a delayed strong increase in b. The effect is modulated by DPPC in the subphase and by cholesterol. Investigations with L-α-lysophosphatidylcholine show the high sensitivity of the ODS technique in the determination of the energy dissipation at air-liquid boundary surfaces. Although the ODS is limited to applications with $\gamma > 15$ mN m^{-1}, it offers the advantage to give, with small samples and within seconds, a simultaneous readout of both surface tension γ and the parameter b, as a measure of surface viscosity.

Key words Surface viscosity · Surface tension · Surfactant lipid

Abbreviations *DPPC* dipalmitoyl phosphatidylcholine · *Lyso-PC* L-α-lysophosphatidylcholine (oleoyl C18:1) · *ODS* oscillating drop surfactometer · *MD* microdrop

W. Meier · G. Greune · A. Meyboom · K.P. Hofmann (✉)
Institut für Medizinische Physik und Biophysik,
Universitätsklinikum Charité, Humboldt-Universität,
10098 Berlin, Germany
e-mail: klaus_peter.hofmann@charite.de

Introduction

We have developed a new apparatus, the oscillating drop surfactometer (ODS), which uses a principle known since more than a century (Rayleigh 1879), extending it to the case of a pendant drop in resonance with an exciter. Our approach is different from existing designs, which use the shape of a pendant drop (Bashforth and Adams 1883), thus allowing the determination of surface tension with high accuracy (Arundel and Bagnall 1977; Bagnall et al. 1978; Lin et al. 1996). By employing the principles of dynamics, the ODS gains additional information on the dissipation of energy in the surface, thus providing an approach to surface viscosity. Actually, viscosity rather than elasticity or surface tension may be the most important determinant for air-water and, specifically, for alveolar interfaces (Hall et al. 1993). In graphic terms, surface tension governs the onset of the movement while the actual deformation will also depend on viscosity. In the currently realized version of the ODS, we form the drop on a small capillary (see Fig. 1) and feed the surface active substance from the subphase, i.e. the interior of the drop, or by injecting microdrops from outside. The instrument needs a very small amount of sample (1 µl) and measures surface tension and frictional damping quasi-simultaneously.

After a first application of the ODS to plasmalogen-containing phospholipid mixtures (Toelle et al. 1999), we have now investigated in more detail the capacity of the instrument, using pure phospholipid, and the complex lipid/protein mixture Survanta from cattle lung. Natural surfactant consists of 90% of lipids and 10% of surfactant-associated proteins (SP-A, SP-B, and SP-C). Phospholipids constitute 96% of the lipids, the major part of which (40%) is dipalmitoylphosphatidylcholine (DPPC). This component is primarily responsible for the lower surface tension of the alveoli, as compared with aqueous solutions (Yu and Possmayer 1996). Other components such as cholesterol may act as fluidizers (Fleming and Keough 1988), while the surfactant

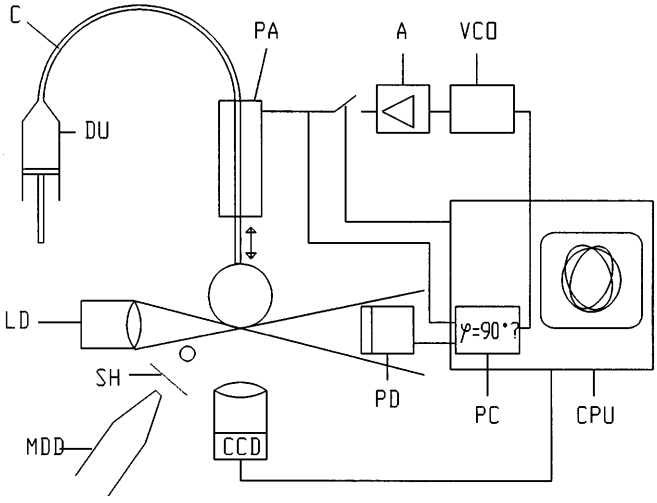

Fig. 1 Schematic diagram of the principal components of the oscillating drop surfactometer (ODS): *A* power amplifier; *C* capillary; *CCD* charge-coupled device camera; *CPU* central processing unit; *DU* dosage unit; *LD* luminescence diode; *MDD* microdrop device; *PA* piezoelectric actor; *PC* phase control; *PD* photodiode; *SH* shutter; *VCO* voltage controlled oscillator

proteins are thought to be involved in the regulation of the transport of phospholipid to and from the air-water interface (Keough 1992; Taneva and Keough 1994a).

A variety of measuring techniques have been developed which allow investigation of the surface tension of fluids containing lipids or lipid/protein mixtures, including the Langmuir-Wilhelmy balance (Clements 1957; Taneva and Keough 1994b) and the Du Noy-Ring (Du Noy 1919). Recent techniques have employed drops or bubbles formed from the liquids under investigation, as for example the pulsating bubble (Adams and Enhorning 1966) or captive bubble (Putz et al. 1994; Schurch et al. 1995; Herold 1997) surfactometers.

In order to avoid detachment of the hanging drop, the application of the ODS is limited to ca. 15 mN/m at the geometry used (Tate's law). The advantage of the system is a time-resolved measurement of both surface tension and frictional damping, using only one microliter of sample.

Materials and methods

Theory

In a force-free space, a fluid body tends to minimize its surface and thus assumes a spherical shape. Any deformation leads to a larger surface and retracting forces which result, together with the inertia of the fluid, in an oscillating system. The addition of a damping term yields the well known equation for a harmonic oscillator:

$$m \times \ddot{x} + b \times \dot{x} + \gamma \times x = 0 \qquad (1)$$

where m is the mass of the drop (kg), b the friction constant (kg s^{-1}) and γ a direction constant, i.e. the surface tension (N m^{-1}); $x(t)$ is a parameter that describes the time-dependent coordinate of deformation.

The harmonic oscillator approximation is valid for sufficiently small amplitudes, i.e. as long as the retracting force resulting from the surface curvature remains proportional to the deformation, x. Lord Rayleigh investigated the free falling liquid drop 120 years ago (Rayleigh 1879). Neglecting frictional effects, he found the following expression for the oscillation period, T_0:

$$T_0 = (3\pi\, m/n(n-1)(n+2)\gamma)^{\frac{1}{2}} \qquad n = 2 \ldots\ n \qquad (2)$$

where n is the order of the mode of oscillation. For an experimental verification, see Lenard (1887).

Real physical systems are damped by a number of frictional influences which lead to a shift of the frequency of oscillation, so that the eigenfrequency of the system is no longer given by Eq. (2). Forced oscillations of the pendant drop allow us to evaluate the case of resonance, in which the frequency of the exciter ω equals the eigenfrequency of the damped system, and the dissipated energy is provided with the optimal phase shift of 90°. In this case, the overall damping of the drop can be determined as follows:

1. From the free decay of the oscillation after shut-off of the exciter. The maxima of the oscillation obey $e^{-\delta t}$, from which δ and thus $b = 2m\delta$ can be obtained. With this method, the analysis of very strong damping ($\delta >$ ca. 30 s^{-1}) is not possible. Figure 2B shows the typical decay of the free damped oscillation measured with the ODS ($\delta = 5.81$ s^{-1}).
2. From the maximum of the resonance curve. It is located at:

$$\omega = \omega_0\left(1 - 2\vartheta^2\right)^{\frac{1}{2}} \qquad (3)$$

with the degree of damping $\vartheta = \delta/\omega_0$. In practice, this method is not applicable in the case of strong damping, i.e. when $\vartheta > 0.04$, because the resulting flat resonance curves do not allow the determination of the maximum with sufficient accuracy.
3. From the phase difference between exciter and oscillator (Fig. 3A). It is given by:

$$\varphi = -\arctan(2\vartheta v/(1 - v^2)) \qquad (4)$$

with $v = \omega/\omega_0$. Thus:

$$\mathrm{d}\varphi/\mathrm{d}v = 2\vartheta\left(1 + v^2\right)\Big/\left((1 - v)^2 + 4\vartheta^2 v^2\right) \qquad (5)$$

and in the resonance case ($v = 1$):

$$\mathrm{d}\varphi/\mathrm{d}v = 1/\vartheta \qquad (6)$$

and thus $b = 2m\vartheta\omega_0$. The degree of damping ϑ determines the slope of the phase shift curve at resonance, so that detuning the exciter allows to determine ϑ and thus b. This will be the method of

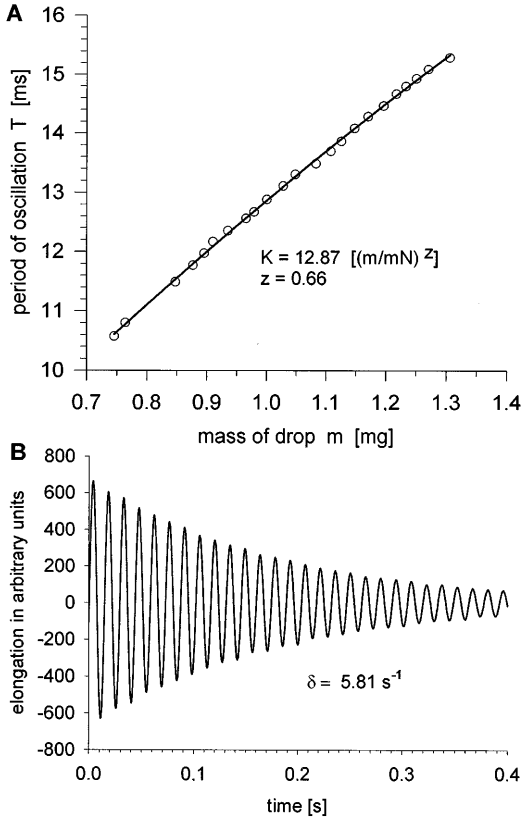

Fig. 2A, B Period of oscillation and damping of a drop in the ODS. **A** Period of oscillation T of a drop in resonance as a function of its mass, for pure water. The *solid line* shows the least-squares fit according to Eq. (7). **B** Typical decay of the free, damped oscillation of a drop formed from saline buffer and covered with DPPC. To account for the transition into the free oscillation, the record (40 kHz sampling rate) shows data points starting from 0.2 s after the stop of the exciter. Using an exponential fit, the damping coefficient is calculated, in this example, as $\delta = 5.81\ s^{-1}$

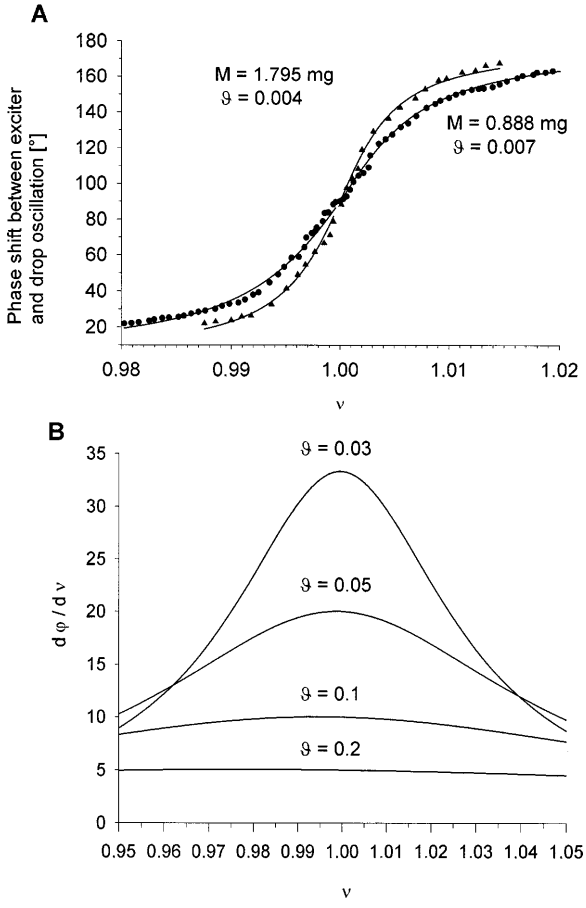

Fig. 3A, B Phase shift between exciter and drop oscillation. **A** Original data of the phase shift φ between exciter and drop in the proximity of the resonant frequency ($\nu = 1$) for two different degrees of damping. In both cases the drop was formed from formamide with different volume (mass). **B** Slope of the phase difference $d\varphi/d\nu$ for different degrees of damping ϑ in the proximity of the resonant frequency ($\nu = 1$) according to Eq. (5)

choice for strongly damped systems, where the other methods are no longer applicable.

Methods 1 and 3 were used in the experiments.

Experimental setup

Formation and control of the drop

The drop (see Fig. 1) is formed on a perpendicular glass capillary (C) with an outer diameter of 239 μm (G 31, MicroFil, World Precision Instruments, USA), in a closed cuvette. A container on the bottom of the cuvette contains a small amount of the fluid from which the drop is formed, leading to a saturated vapour atmosphere. The amount of fluid used to form the drop (typically ca. 1 μl) is adjusted by a programmable dosage unit (DU) (Microlab 500, Hamilton, Bonaduz, Switzerland); doses are applied in steps of 50 nl. The capillary is set vibrating by a cylindrical, piezoelectrical actor (PA) (HPSt 150/14-10/25, Piezomechanik, Dr. Lutz Pickelmann, München, Germany), leading to axial oscillation of the capillary and thus of the pendant drop.

The exciter frequency is generated by a voltage controlled oscillator (VCO), in which the frequency determining DC voltage is programmable via the D/A exit of the D/A-A/D module (AT-MIO-16E-10, National Instruments, Austin, USA). The mechanical eigenfrequency of the actor (44 kHz) is far off the frequencies used (40–100 Hz). The system allows correction of the internal phase shifts in the exciter system.

The drop is observed and controlled by an imaging system, with a large luminiscence diode providing a bright background, and a CCD camera (C 2400-75 ICH, Hamamatsu Photonics, Japan). Images are evaluated using the system Argus 20 (Hamamatsu Photonics, Japan) and a data processing unit (with Frame-Grabber Screen-machine, 640×512 pixels, Fast Electronics, München, Germany). From the contour of the drop, obtained by the video-image processing system, the volume and mass of the drops are calculated, using known algorithms. The accuracy is within $\pm 0.5\%$ for

volume and area, calibrated with a spherical standard object.

To measure the oscillation of the drop, the light emitting area of an IR luminescence diode (LD) is projected with a lens onto the lower part of the drop. The shadow of the drop partially covers a square PIN photodiode (PD). Oscillation of the drop leads to light modulation, which is measured the PD. A quasi-sinusoidal voltage signal is obtained, which is fed into an A/D converter and evaluated in the CPU.

Adjusting the resonance case

The resonance case ($v = 1$, $\phi = 90°$) is adjusted by regulating the phase difference between exciter and oscillator. Both signals are sampled with 40 kHz over a time interval from 0.1 s, so that in the relevant frequency range (40–80 Hz) more than 1000 sampling points are available with an amplitude resolution of 12 bit.

The software for adjusting the phase difference was developed on the basis of LabWindows CVI (National Instruments, USA). Each adjustment takes one second; during this time, the phase difference (difference between zero passages of both signals) is compared with the nominal value (90°), and a proportional voltage is generated which is fed into the VCO. The algorithm is adaptive such that any measurement of the damping constant optimizes the approach procedure due to the estimation of the slope of Φ (v) at $v = 1$. Typically, the nominal value is reached after four measuring cycles (for an initial deviation $\Phi < 30°$). All relevant parameters, as for example the exciter amplitude, can be adjusted during the experiment.

Microdrop injection

To cover the surface of the oscillating drop with lipid, a piezomechanical microdrop device (MDD in Fig. 1; Microdrop, Norderstedt, Germany) is employed. The microdrops (MDs) serve in our experiments as the carrier of the surface active substances. To calculate the actual transported quantity of lipids, one has to know the concentration of the solution and the volume of the MD after formation at the mouth of the MDD. Different influences are expected to affect the actual amount of substance that reaches the oscillating drop surface. On the one hand, the high vapour pressure at the surface of the MD, caused by the small radius of curvature [see Eq. (10) below], leads to an evaporation of solvent during the flight time of the MD to the oscillating drop. On the other hand, a flying MD moves in the vapour hose of the ahead-flying MD, so that the effect is reduced. Because the small mass and the high evaporation rate of the MDs makes a determination by weighing of the "true" size of the MDs impossible, three independent measuring procedures were applied, namely:

1. Electronic pictures from MDs were grabbed under stroboscopic lighting with 500-fold enlargement and measured by image processing with the Scion Image Software for Windows 95 (Scion, Frederick, Md. USA). The scale was calibrated using an etalon by Carl Zeiss, Germany. The emitted MDs have a diameter in the case of water of 70.2 $\pm$ 0.8 μm ($n = 14$) and 69.7 $\pm$ 1.4 μm ($n = 14$) in the case of a chloroform/methanol solution (2:1), and thus a calculated volume of 181 pl and 178 pl, respectively.
2. The enlargement of the volume of the oscillating drop after injection of 1000 MDs was calculated from its contour, as described above. The volume of one single MD was determined as 180.38 pl $\pm$ 10.17 pl ($n = 10$) for water.
3. Any change in the mass of the oscillating drop leads in accordance with Eq. (7) (below) to a change of the oscillation duration T. A series of 100 MDs were injected into a drop, oscillating in resonance, and the drift of the oscillation period determined. From this procedure the volume for one MD was determined as 182.74 $\pm$ 3.17 pl ($n = 45$) for water.

In principle, the free oscillations of an MD could also be used to calculate its mass. However, the relatively large amplitude of these oscillations leads to non-linearities and an increase of the oscillation period (Trinh and Wang 1982; Wang et al. 1996; Tian et al. 1997), so that this procedure for the determination of mass of the MD could not be used. On the other hand, the procedures 1–3 above yield sufficient and consistent information. For practical reasons the optical measurement (1) was routinely applied. Since the size of the microdrops depends on surface tension and viscosity, it must be controlled separately in each experiment.

Because the surface active substances are solved in an easily vaporizing solvent (e.g. DPPC in chloroform/methanol), the concentration of the solved material may also change by evaporation of the solvent at the top of the MDD. Therefore, some microdrops were routinely fired onto a shutter (SH) before starting the experiment, so that the subsequent drops have the concentration of the stock solution. MDs can be applied as single shots or in rapid succession (maximally 2000 MDs per second).

Preparations and materials

Fluids

Pure water was purchased as double-processed tissue culture water from Sigma, and isotonic NaCl solution from Fresenius (Bad Homburg, Germany). Formamide, ethylene glycol, and nitromethane were purchased from Fluka (Deisenhofen, Germany) and used without further purification. Values for the physical properties were obtained from Lide (1998). Surface tension was addi-

tionally controlled using Axisymmetric Drop Shape Analysis (ADSA) (Chen et al. 1998a).

All experiments were performed at 20 ± 1 °C.

Liposome preparation

All lipids purchased from Sigma were used without further purification; the purity of DPPC, lyso-PC, and cholesterol was 99%. Phospholipid mixtures in methanol:chloroform (1:2), consisting of dipalmitoylphosphatidylcholine/cholesterol (9:1 and 1:1) were dried under vacuum using a Speed Vac system (Eppendorf, Engelsdorf, Germany). Lipid films were hydrated at 50 °C in a Tris buffer (5 mM Tris, pH 7.4, containing 100 mM NaCl and 50 μM EGTA), adjusted to a phospholipid concentration of 10 mg/ml and vigorously shaken.

Survanta, a phospholipid fraction from cattle lung was purchased from Abbott (Wiesbaden, Germany) and diluted in Tris buffer.

Multilamellar liposomes were obtained by 10 repeated freeze-thaw cycles. Subsequent extrusion through a polycarbonate membrane of 200 nm or 50 nm pore size, using a Liposo-Fast extrusion set (Avestin, Ottawa, Canada) yielded unilamellar liposomes (MacDonald et al. 1991).

The PC content of lipid samples was analyzed using the Stewart assay (Stewart 1980).

Drop size, oscillation amplitude, and lipid injection

The optimal drop size is a compromise: on the one hand, very small drops evaporate rapidly (note that convex surfaces are not in equilibrium with their atmosphere); on the other hand, the surface properties we are interested in dominate the smaller the drop. Except for calibration, the volume of the drops was chosen to be 1–1.05 μl, and thus the surface ca. 4.8 mm^2. The glass capillaries had an external diameter of 239 μm.

To meet the conditions of Eq. (1) and to keep the overall dissipation of energy low within the drop and on its surface, the oscillation amplitude should be kept as small as possible. Thus nonlinear effects are avoided, as they occur with large amplitudes [> 15% of the drop diameter (Wang et al. 1996)]. In the routinely employed mode of operation, the amplitude of oscillation at the lower drop edge was generally smaller than 2% of the drop radius.

From the lipid solutions applied, one obtains a volumetric value for the number of lipid molecules per microdrop and thus a measure of surface density of lipid on the oscillating drop (usually given as area per molecule, e.g. for experiments with a Langmuir trough). We have found, however, that the physical effect of these molecules on a moving surface is changed, compared to static conditions. We therefore give "apparent dynamic" values of surface density (see Results).

Experimental tests

Correction for capillary fixation and loss of mass

The oscillation of a hanging drop is disturbed by the fixation of part of the surface, the reduced oscillating surface, and by the oscillation of the centre of mass, compared with the freely falling drop. Experiments with various liquids have shown that a pendant drop with mass m oscillates at resonance with a period

$$T = Km^z \tag{7}$$

where $z \neq 0.5$ [compare Rayleigh's case, Eq. (2)]. Figure 2A shows as an example the dependence of the period of oscillation T on the mass of the drop, formed from pure water. The data points are fitted using Eq. (7). K can be interpreted as the period of oscillation of a drop of mass 1 mg.

Introducing the term $k = 3\pi/n(n-1)(n+2)$ in Rayleigh's solution [Eq. (2)], the constant K can be written as

$$K = \left(k \Big/ \gamma\right)^z,$$

in which k is a constant and γ is surface tension. Under the conditions of our measurements, the fundamental mode of oscillation ($n = 2$) is used. Assuming that k and z are independent of γ (Bisch et al. 1982), and for otherwise constant parameters (for example, the same diameter of the capillary), γ can be calculated for any other fluid, when m and T are known at the time t:

$$\gamma(t) = \left(T_{H_2O}/T(t)\right)^{\frac{1}{z}} \gamma_{H_2O} m(t) \tag{8}$$

This expression includes the case that the mass varies slowly (as compared to T) during the time of the measurement. In a set of experiments using drops of 1 mg water, we obtained for $T_{H_2O} = 12.89 \pm 0.12$ ms, $z = 0.66 \pm 0.02$ ($n = 15$).

The surface tension as function of the oscillation duration, calculated by means of Eq. (8), is shown in Fig. 4A (dotted line). We went on to check the prerequisite for the validity of Eq. (8), namely, whether the constants k and z are independent of surface tension. For a selection of Newtonian liquids with well-known surface tension (formamide, ethylene glycol, and nitromethane), the period of oscillation was generally smaller than predicted from Eq. (8) (Fig. 4A). Using the same mathematical model, we can well fit these values with the function $\gamma = 12001.5/T^{2.042}$. In the examined range of surface tension, a linear correlation exists between the experimentally found values and those which were calculated by means of Eq. (8) (see Fig. 4B). This leads to Eq. (9):

$$\gamma(t) = 1.161\left(T_{H_2O}/T(t)\right)^{\frac{1}{z}} \gamma_{H_2O} m(t) - 11.970 \tag{9}$$

Using Eq. (9), it can be shown that the relative error in the determination of the mass of the drop, $\Delta m/m$, is the

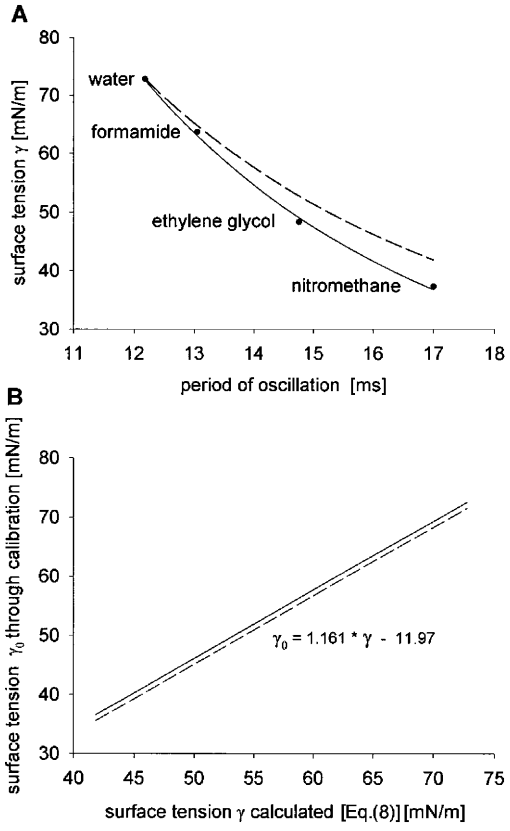

Fig. 4A, B Calibration of surface tension, based on the experimentally determined period of oscillation, for drops with mass 1 mg, formed from different substances. **A** Period of oscillation T, with different fluids, and non-linear least-squares fit (*solid line*; power function $12001.5/T^{2.042}$). The *broken line* shows the calculated surface tension γ for water, using the function $3210.61/T^{1.515}$ [Eq. (8)]. **B** Functional relationship between γ_0 (from calibration in Fig. 4A) and γ [Eq. (8)]. In the experimentally examined range, γ_0 and γ are proportional to each other with good approximation (coefficient of regression $R = 0.99992$), justifying a linear correction factor [see Eq. (9)]. For better visibility, the fit function (*broken line*) is vertically shifted (by −1 mN/m)

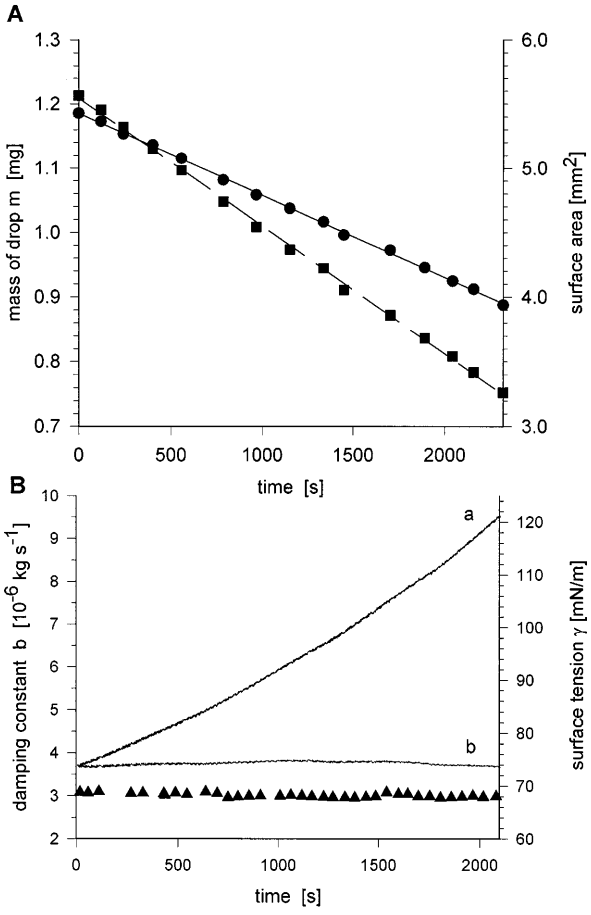

Fig. 5A, B Effect of evaporation. **A** Loss of mass (*filled squares*) and surface (*circles*) of a small drop of water by evaporation in a highly saturated vapour atmosphere, as a function of time. **B** Time course of surface tension [Eq. (9); line *a*] and time course corrected for the loss of mass (line *b*). The *triangles* show the corrected time course of the damping constant b (frequency range in this experiment 68.46–94.99 Hz)

same as that of surface tension ($\Delta\gamma/\gamma$). In practice, this will result in a relative error of $\pm 1\%$. On the other hand, errors in the determination of the oscillation time T ($< 0.1\%$) have less influence on the resulting value of γ.

Correction for loss of mass

Although the drop is formed in a closed cuvette, it is not in equilibrium with its own atmosphere. Owing to its curved surface, there is a vapour pressure difference given by:

$$\Delta p = 2pV\gamma/RTr \qquad (10)$$

where V is the molar volume, γ the surface tension, and r the radius of the drop. This leads to a slow evaporation of the drop.

Under the conditions of the experiments, the oscillating drop loses mass and surface area by evaporation (Fig. 5A). During the 40 min of the experiment the loss of mass, taken from the linear least-squares fit to the data (broken line), was 19.83×10^{-5} mg/s and the accompanying decrease in surface 63.82×10^{-5} mm^2/s. This phenomenon requires us to correct, in each experiment, the mass of the drop according to Eqs. (8) and (9). Figure 5B shows the apparent increase of γ with time, for a drop formed from pure water. With the mass correction according to Eq. (9), γ remains, as expected, fairly constant (note the expanded scale), in this example 74.21 ± 0.41 mN/m (mean of 2095 data points in Fig. 5B). With the corrected mass, the same constancy is seen for the damping constant b (filled triangles); in this special case, $\bar{b} = 3.04 \pm 0.12 \times 10^{-6}$ kg/s (37 data points).

Surface and bulk viscosity

Any change in the shape of a drop can only occur by liquid motion. This leads to energy dissipation by in-

ternal friction. On the other hand, this deformation is possible only by an enlargement of the surface.

While with a sphere the deformation of the surface is exclusively effected by dilatation or compression (i.e. by a change of volume), with the oscillating drop an additional shear deformation must necessarily occur. Both generate a dilatational and shear flow, which is restricted by surface dilatational viscosity and surface shear viscosity (Chen et al. 1998b). In principle, we cannot differentiate between components of overall dissipation, such as bulk and surface viscosities, or even air friction. However, if small drops are employed, properties of the surface dominate because of the favorable surface/volume ratio.

For the experimental determination of the damping factor b [Eq. (1)], two different methods were used. At sufficiently small b ($\delta <$ ca. 40 s^{-1}, mass = 1 mg) the decay curve of the oscillation was recorded (see Fig. 2B) and δ determined using a non-linear fitting procedure for the amplitudes. If the loss of energy is too large, sufficient data are no longer available for the analysis and another method was used. In these cases the phase angle relative to the case of resonance is evaluated, which occurs by any detuning of the oscillator. The degree of damping ϑ was then calculated according to Eq. (6).

$d\phi/d\nu$ has a relative maximum in the resonance case ($\nu = 1$) (Fig. 3B). If $\Delta\nu$ is small enough, one can determine this maximum with sufficient accuracy. In our experiments, $\Delta\nu$ was selected in such a way that a phase shift of $\Delta\phi < 10°$ occurred. In a real experiment, this corresponds, with a relative frequency shift $\Delta\nu = 0.006$ and at a resonance frequency of 52.79 Hz (damping constant $b = 75.6 \times 10^{-6}$ kg/s, degree of damping $\vartheta = 0.026$), to a phase shift of $\Delta\phi = 5.2°$.

There are also specific reasons to assign the measured damping to the surface rather than the bulk. For example, it is known that DPPC in organic solution, injected from outside, does not significantly redistribute into the bulk, so that its effect on surface damping dominates. More importantly, liposomes suspended in the bulk do not measurably change the damping constant, as compared to pure saline. As will be shown below, a pronounced frictional damping develops only in the course of lipid transport to the surface. Since the surface properties may depend on the deformation rate, the frequency range used is indicated in the figures.

From a number of independent determinations, one obtains for pure water $\bar{b} = (2.906 \pm 0.077) \times 10^{-6}$ kg/s ($n = 69$), and for 5 mM Tris buffer, a significantly higher value, namely $\bar{b} = (3.189 \pm 0.060) \times 10^{-6}$ kg/s ($n = 73$) ($P < 0.001$).

Results

Survanta liposomes

Survanta is a complex mixture of phospholipids, fatty acids, and hydrophobic surfactant proteins, obtained from bovine lung. Its main constituents are DPPC (approx. 48%), phosphatidylcholine (approx. 16%), phosphatidylglycerol (approx. 4%), and other lipids, and low amounts of hydrophobic surfactant proteins (SP-B and SP-C). In contrast to pure DPPC (see below), Survanta liposomes adsorb spontaneously to the freshly formed surface of the pendant drop. This is obvious from the time-dependent decrease in surface tension and increase in damping, which both start immediately after forming the drop. Figure 6 shows this for two concentrations.

The adsorption of Survanta to the surface proceeds with a rate that depends on the concentration (dominant rates 1.4 and 1.9×10^{-3} s^{-1} at 1000- or 500-fold dilution, respectively). In both cases, liposome adsorption drives surface tension to approx. 40 mN/m. This is accompanied by an almost threefold rise of the damping constant, with a characteristic delay to surface tension. Although a mechanism for this behaviour can not be envisaged, it seems to be clear that surface damping and tension depend on different molecular determinants.

DPPC injection induces the uptake of subphase liposomes into the surface

Surface tension decreases when DPPC in organic solution is injected into the oscillating drop. Fifteen microdrops, transporting approx. 20×10^{11} molecules and leading to a mean area per molecule of about 220×10^{-20} m^2, lower the surface tension of a drop formed from Tris buffer to approximately 55 mN/m. The original protocol of this experiment is shown in Fig. 7A. As expected for the limited amount of injected

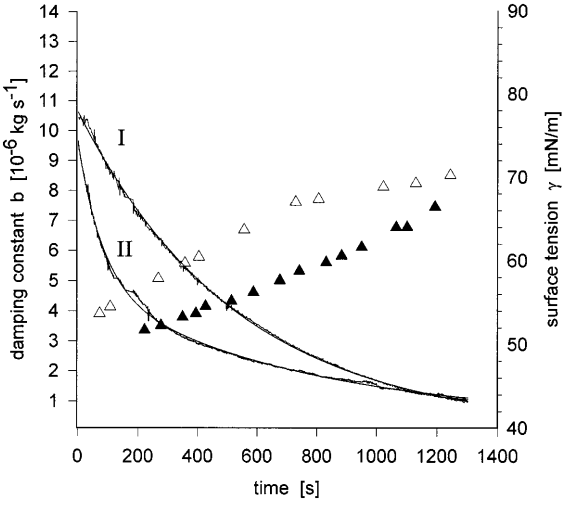

Fig. 6 Effect of Survanta on surface tension and damping of the ODS oscillating drop. The drop is formed at $t = 0$ from a suspension of liposomes (200 nm diameter) in 5 mM Tris buffer; spontaneous adsorption to the surface leads to a temporal change of surface tension γ (*solid lines I and II*, PC 19.5 μg/ml and 39.0 μg/ml, respectively) and damping constant b (*filled and open triangles*)

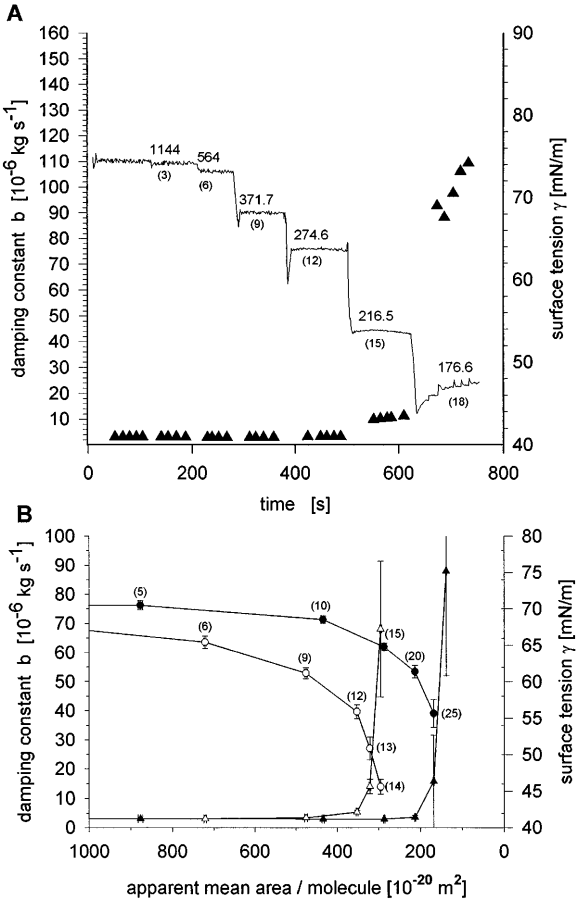

Fig. 7A, B Effect of DPPC on surface tension and damping of the ODS oscillating drop. **A** The drop is formed at $t = 0$ from Tris/NaCl solution (see Materials and methods). Microdrop injection of DPPC solution leads to changes of surface tension γ (*solid line*) and damping constant b (*triangles*, frequency range 80.75–69.91 Hz, original data). *Numbers* at the steps indicate the total number of injected drops (in parentheses) and the mean area per molecule (10^{-20} mm^2) reached after each injection (one microdrop contains 1.4×10^{11} molecules; see Materials and methods). **B** Surface tension and damping in the presence (*open circles*) and absence (*filled circles*) of DPPC liposomes in the interior of the oscillating drop. Plot of surface tension γ (*circles*) and damping constant b (*triangles*, frequency range 79.72–66.99 Hz) as a function of the mean surface area occupied per molecule injected. *Numbers in parentheses* indicate the total number of injected microdrops, containing 1.09×10^{11} molecules each. Each data point and standard deviation is from three independent measurements

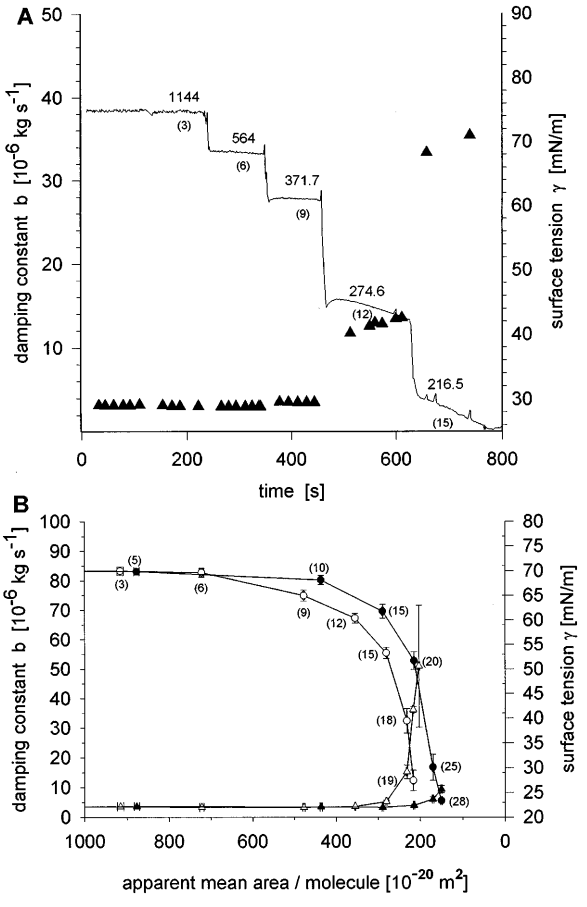

Fig. 8A, B Effect of DPPC and cholesterol on surface tension and damping of the ODS oscillating drop (original data). **A** The drop is formed at $t = 0$ from a suspension of DPPC/cholesterol (9:1) liposomes (50 nm diameter) in Tris/NaCl solution. Microdrop injection of DPPC solution leads to changes of surface tension γ (*solid line*) and damping constant b (*triangles*, frequency range 80.58–52.93 Hz, original data). *Numbers* at the steps indicate the total number of injected drops (in parentheses) and the mean area per molecule (10^{-20} mm^2) reached after each injection (1.4×10^{11} molecules per microdrop; see Materials and methods). **B** Surface tension and damping of a drop formed from DPPC/cholesterol suspension (9:1, *open symbols*; 1:1, *filled symbols*). Plot of surface tension γ (*circles*) and damping constant b (*triangles*, frequency range 80.00–46.86 Hz) as a function of the mean surface area occupied per molecule (10^{-20} mm^2) injected. The *numbers in the parentheses* represent the number of injected drops containing 1.4×10^{11} molecules (see Materials and methods). Each data point and standard deviation is from three independent measurements

molecules, the surface tension assumes a constant value after each injection. The increase in energy dissipation is dramatic, as seen from the rise of the damping constant by a factor of 30, compared to the freshly formed drop.

When the DPPC lipid was present in the subphase in form of liposomes (of approx. 50 nm diameter), no significant change in surface tension or damping was observed for 10 min, for dispersions of different concentration and salt composition (data not shown). To find out whether small amounts of DPPC in the surface would act as adsorption nuclei, thus inducing adsorption, we injected microdrops of DPPC with liposomes simultaneously present in the subphase. As is shown in Fig. 7B, only half of the number of microdrops is necessary to suppress surface tension to the same value and to enhance surface damping to the same degree as above, indicating that lipid from the subphase indeed contributes to surface activity. No effect is seen when pure solvent is injected (data not shown).

The effect of cholesterol

When liposomes with 10% cholesterol are used, microdrop injection of pure DPPC induces liposome uptake as above (Fig. 8A). However, the damping constant is much

smaller for a given value of surface tension (Fig. 8B), although the overall decrease of surface tension is similar (Fig. 7B). When the fraction of cholesterol in the liposomes is further enhanced, the surface damping of the lipid film is further reduced, and reaches with 7×10^{-6} kg/s, only twice the magnitude as without any lipid.

For a sufficiently high amount of injected DPPC, surface tension continues to decrease after the initial step following each injection, with a concomitant rise of damping. This behaviour starts after injection of 6 and is most obvious with 12 and 15 microdrops.

Properties of lyso forms of phospholipids

For lyso forms of phospholipids, such as lysophosphatidylcholine and lysophosphatidylserine, Evans and co-workers (Evans et al. 1980) could not find any difference in the surface viscosity of pure water. This was measured in the range of surface pressure between 2 and 30 mN/m and using an oscillating pendulum method. We therefore decided to test the sensitivity of our method with respect to surface viscosity, applying oleoyl-lysophosphatidylcholine (Lyso-PC).

Similar to DPPC, the surface tension decreases when Lyso-PC in organic solution is brought to the oscillating drop surface by successive microdrop injection. The surface tension as a function of the apparent dynamic area per molecule is shown in Fig. 9B. The surface tension at equilibrium amounts to 34.21 ± 0.01 mN/m ($n = 3$). Surprisingly, however, the surface damping parameter b remains, over a large range of surface density, below the base value of the uncontaminated fresh water surface (3.31×10^{-6} kg/s^2). The effect is seen with the DPPC/cholesterol system (Fig. 9A, enlargement of Fig. 7B) and, most significantly with the Lyso-PC system, when the area/molecule value becomes lower than 160×10^{-20} m^2. Surface damping returns to its starting value when surface tension adopts its equilibrium value. Although the qualitative behaviour is the same in different experiments, within the region of the steepest slope, very small differences in the average area/molecule cause distinct differences in γ (as seen in the relatively large standard deviations), while surface damping remains almost constant.

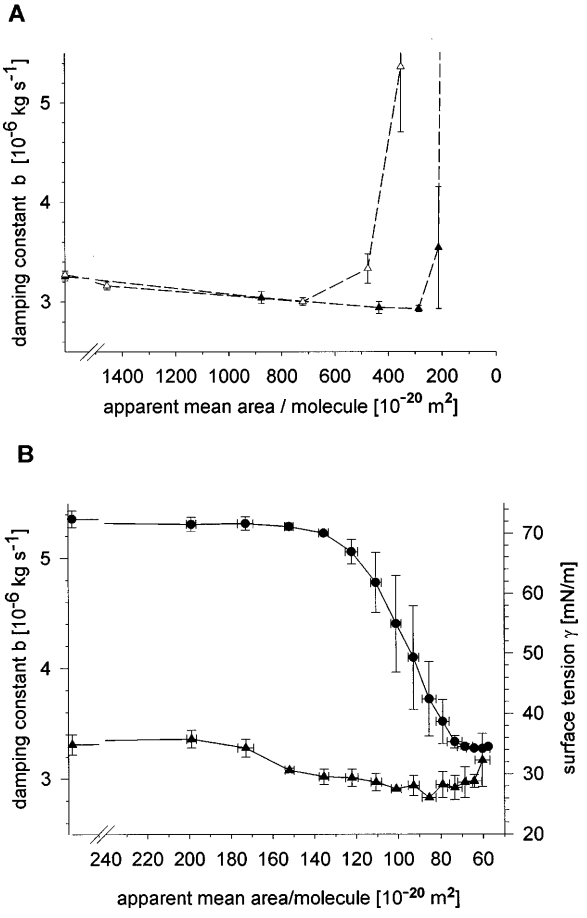

Fig. 9A, B Decrease of damping at low surface concentration. **A** Effect of DPPC on the damping constant of an ODS drop. Damping constant b in the presence (*open*) and absence (*filled*) of DPPC liposomes in the interior of an oscillating drop; data are from Fig. 7B, and shown on a larger scale. **B** Surface tension γ (*circles*) and damping b (*triangles*) of a drop injected with lyso-PC via microdrops. Each point represents the mean of three experiments. *Horizontal* and *vertical bars* are standard deviations. The data points near the ordinate were measured with pure water

Discussion

Main characteristics of the new technique

It has long been known that the frequency of oscillation of a freely falling drop is a most sensitive and non-invasive parameter to study surface properties (Lenard 1887). The principle has later been realized in the form of a "levitated" drop, in which the drop is suspended by electromagnetic (Sauerland et al. 1993; Egry et al. 1996) or sound fields (Achatz 1977; Trinh and Wang 1982; Tian et al. 1997). By computer modelling, Tian et al. have found ways to determine the phase shift between the exciter signal (modulation signal of the sound field) and the oscillation of the levitated drop.

By employing a capillary, both to form and to excite the drop to resonance oscillations (identified by the phase condition $\Delta\phi = 90°$), the oscillating drop surfactometer (ODS) allows measurement of surface tension and energy dissipation independently and simultaneously. The determination of the phase shift is in this case very simple, the drop can be kept in the resonance condition, and the damping constant can be measured even in cases where the free decay of the damped oscillation cannot be used. As this study shows, the ODS can provide complementary information to the more established techniques [see the Introduction and (Franses et al. 1996)]. Of course, the main advantage of the ODS is that it uses a minute amount of sample.

The π-A isotherm of lipids in the ODS

The π-A isotherm of lipids shows a typical coexistence region between the liquid expanded (LE) and liquid condensed (LC) phases. It is best observed by compressing a lipid film starting from the gas phase (Möhwald 1993). The phase transition between the LE and LC phases reflects itself (for DPPC at room temperature) in a more or less expressed plateau between 5 and 10 mN/m. The plateau depends on the purity of the lipid and on the finish of the film (Möhwald 1993). In the literature, the beginning of the LE phase generally occurs in the range of 90–110×10^{-20} m^2, and the transition into the LC phase at ca. 57–60×10^{-20} m^2 per lipid molecule. At further compression, a steep rise of surface pressure occurs in the 45×10^{-20} m^2 range, which is interpreted as the transition into the solid condensed (SC) (Denicourt et al. 1989; Möhwald 1993; Denicourt et al. 1994; Li et al. 1996a).

In our measurements (see Figs. 7B and 8B) we find interesting differences to the behavior of lipid layers in the Langmuir trough:

1. The plateau indicating the coexistence phase is lacking. The same observation was made by Li and coworkers (Li et al. 1996b), using the axisymmetric drop shape analysis (ASDA). These authors interpreted the effect by a slowed nucleation process in a curved surface so that, within the range of the compression rates applied, an equilibrium is not achieved. It is conceivable that, with the even higher compression rates in the ODS, this effect is even more expressed. It was also considered that, because of the (compared to the surface) small bulk phase, lipid impurities become more effective, thus preventing the expression of a plateau, which requires the coexistence of only two pure components (Miller and Möhwald 1987).
2. The first rise of the resonance oscillation period (reflecting a decrease of surface tension) occurs at much lower concentration of lipid, in the range of 600–800×10^{-20} m^2 per lipid (assuming monomolecular dispersion). This is a 10-fold lower lipid density than the one at which the first deviation from the baseline becomes measurable in the Langmuir trough and the ADSA.
3. The well-known steep decrease of surface tension, which is interpreted as the end of the coexistence phase, occurs earlier with the ODS, typically with twice the mean surface area/molecule, as compared with the trough.

An obvious explanation for phenomena 2 and 3 would be that more lipid is transported per MD than was calculated from concentration and volume. However, such an artefact would not explain the different scaling for the two effects. Moreover, the experimental precautions and the careful determination of the MD volume make it unlikely to occur (see Experimental set-up). A better explanation is offered from the observation in epifluorescence microscopy (Miller and Möhwald 1987; Nag and Keough 1993; Kretzschmar et al. 1996; Worthman et al. 1997) that, in pure DPPC monolayers, small liquid crystal domains form at relatively low surface pressure, which grow with increasing surface pressure. It seems conceivable that the nucleation process for the generation of such domains, and their following growth, begins under our dynamic conditions with smaller quantities of lipid, as compared with a resting surface.

Although the reasons remain to be elucidated, it seems clear that the reactivity of the ODS to small amounts of lipid is not due to miscalibration but to a real physical effect. Nevertheless we will use "apparent dynamic" units for the lipid concentration, to indicate that they are formally calculated units of mean area/molecule, as they are used in the literature.

Oscillation damping and viscosity

Kraegel and co-workers (Kraegel et al. 1996) report for DPPC an increase of surface shear viscosity (frequency 0.1 cycles per second) beginning from zero surface pressure up to ca. 10 mN/m, i.e. the end of the coexistence phase. Above a surface pressure of ca. 32 mN/m a stronger rise was observed, leading to the proposal of a further phase transition not accessible to measurements of surface tension alone. The same authors also observe saw a strong rise of the surface dilatational viscosity outside the assumed LE/LC phase.

In Fig. 7B, and even more expressed in Fig. 9A, a drastic modification of the damping constant b can be likewise observed with the ODS. In accordance with Kraegel et al., we find a rise of the damping constant b with increasing surface lipid density. The rise is even more abrupt than in their measurements, which is most probably due to the higher frequency range in our experiments (non-Newtonian behaviour). The increase in energy absorption of the system could be due to an increasing displacement of water from the DPPC polar head groups (Denicourt et al. 1994).

Damping at low lipid density

All experiments with the ODS have one surprising observation in common, namely, a small but significant reduction of damping at low density of lipid (area per molecule $> 200 \times 10^{-20}$ m^2; Fig. 9A and B). This phenomenon always preceded any measurable change of the oscillation period (reflecting surface tension γ).

With DPPC, the base value of the surface damping of a newly formed and uncontaminated surface is, after its initial decrease, only adopted again when the surface tension for a lipid film has dropped by at least 10 mN/m (Fig. 7B). When cholesterol is added and surface damping is generally lowered, damping rises beyond the base value only with a much larger decrease of surface tension (e.g. > 20 mN/m in Fig. 8B). With Lyso-PC, the damping parameter does not return to its base value, even with the equilibrium surface tension of ca. 32 mN/m.

We believe that this substance-specific rise of surface damping must be considered in close relation with its general decrease at low density. We speculate that the short-range order caused by the molecular properties of water is disturbed by the presence of surface active substance. Thereby, specific structures could be formed, in which less energy is dissipated. This idea was already discussed by Blank and Soo (1976), in order to explain the viscosity-lowering effect of cholesterol. Considering in addition the LC domains discussed above, obtained with fluorescence microscopy (Discher et al. 1999), one may conclude that even after the formation of larger LC domains the energy that dissipates into the surface remains low as long as the domains do not collide. Only after the end of the LE/LC coexistence phase, and in the transition to the LS phase, surface damping is expected to assume positive (with respect to very low concentration) values. This would mean that Lyso-PC (Fig. 9B) does not go through a phase transition under these conditions. Further investigations on lysolecithin are under way.

Exchange of lipids with the surface

It can be anticipated that that a precise assignment of the effects measured with the ODS to individual phases of π-A isotherm will require the simultaneous application of optical techniques such as epifluorescence (Nag et al. 1996a; Worthman et al. 1997). On the other hand, the results have shown that the ODS technique provides new sensitive tools to investigate lipid surfaces on water. Future application may include the anchoring of proteins to lipid monolayers. We have recently performed such an investigation on the G-protein of the visual cascade, transducin (Seitz et al. 1999), using the Langmuir trough. The very small sample volume of the ODS may allow future studies to yield more extended and, because of the short diffusion times, kinetically more relevant information.

The current application example was an investigation of artificial lung surfactant and its interaction with the air-water interface. Although the ODS is limited to surface tension above ca. 20 mN/m, in order to avoid detachment of the oscillation drop from the anchoring capillary, some interesting observations could be made.

During respiration and alveolar movement, the incorporation into and release from the alveolar surface must be accomplished on the time scale of respiration. In agreement with the literature, we find that Survanta liposomes (Fig. 6) readily cover the surface in a spontaneous fashion. This had been seen from both a dose-dependent decrease of surface tension and an increase in energy dissipation.

Remarkably, pure DPPC liposomes suspended in the subphase of a lipid monolayer virtually do not exchange with the surface and are thus incapable of developing surface activity under our conditions; see also Meban (1981) and Nag et al. (1996b). Our experiments have shown that, when DPPC is first brought to the surface through microdrop injection, and liposomes are present in the subphase, extra DPPC appears on the surface. Evidence for this notion comes from the significantly (50%) lower surface tension, as compared to injection in the absence of subphase liposomes (Fig. 7B).

Previous work has suggested that aggregates, possibly of linear geometry (Evans 1995), of saturated DPPC are formed at the air-water interface. Such islands of lipid may act as nuclei for the incorporation of lipid from the subphase.

When the subphase liposomes contained cholesterol, both surface tension and damping were specifically altered. Again, the injected lipid induces the incorporation of liposomes into the surface, but the effect of DPPC is lowered by cholesterol in a dose-dependent manner (Fig. 8B). Generally, cholesterol smoothens the effect of the lipid, and more DPPC has to be injected to obtain the same surface activities. Moreover, DPPC induces a specific effect, namely that surface tension continues to fall spontaneously after the initial step following each injection. Apparently, the cholesterol/lipid mixture can mimic to a certain degree the dynamic behaviour of the more complex Survanta mixture (Fig. 6). The effect is the more pronounced the more (injected) lipid is already occupying the surface, and is accompanied by an increase in energy dissipation (Fig. 8A). This is interesting in the light of previous findings that cholesterol acts as a fluidizer (Blank and Soo 1976; Fleming and Keough 1988; Ladha et al. 1996; Worthman et al. 1997) and lowers surface viscosity, as compared to pure DPPC (Evans et al. 1980; Evans 1995). These experiments yield independent evidence that liposomes from the subphase can reach the surface when it is inoculated with lipid. It will be interesting to investigate this effect in the presence of defined amounts of surfactant proteins. In view of the role of cholesterol as a modulator of membrane protein-lipid interaction (Mitchell et al. 1990), these proteins may exert their regulatory effects on the air-water interface of the lung in concert with cholesterol.

Acknowledgements We thank Alexander V. Makievski (Max Planck Institute of Colloids and Interfaces, Berlin) for ADSA calibration measurements and Dieter Maretzki (IMPB) for discussions, and Andreas v. Garnier and Thomas Penczok for technical assistance. This work was supported by the Bundesministerium für Bildung und Forschung (BMBF/FoSped Programm).

References

Achatz M (1977) Verfahren und Vorrichtung zur Bestimmung von Dichte, Oberflächenspannung und Viskosität an kleinen Flüssigkeitsvolumina. Ger Pat 2709698

Adams FH, Enhorning G (1966) Surface properties of lung extracts. Acta Physiol Scand 66: 23–42

Arundel PA, Bagnall RD (1977) The surface area of pendant drops. J Phys Chem 81: 2079–2085

Bagnall RD, Annis JA, Arundel P (1978) A novel technique for studying the adsorption of plasma proteins on hydrophobic surfaces. J Biomed Res 12: 653–663

Bashforth F, Adams JC (1883) An attempt to test the theories of capillary action. Cambridge, University Press, Cambridge

Bisch C, Lasek A, Rodot H (1982) Comportement hydrodynamique de volumes liquides sphériques semi-libres en apesanteur simulée. J Méc Théor Appl 1: 165–183
Blank M, Soo L (1976) The effect of cholesterol on the viscosity of protein-lipid monolayers. Chem Phys Lipids 17: 416–422
Chen P, Kwok DY, Prokop RM, del Rio OI, Susnar SS, Neumann AW (1998a) Axisymmetric drop shape analysis (ADSA) and its applications. In: Möbius D, Miller R (eds) Drops and bubbles in interfacial research. Elsevier, Amsterdam, pp 61–138
Chen XH, Shi T, Tian YR, Jankovsky J, Holt RG, Apfel RE (1998b) Numerical simulation of superoscillations of a triton-bearing drop in microgravity. J Fluid Mech 367: 205–220
Clements JA (1957) Surface tension of lung extracts. Proc Soc Exp Biol Med 95: 170–172
Denicourt N, Tancrede P, Brullemans M, Teissie J (1989) The liquid condensed diffusional transition of dipalmitoylphosphoglycerocholine in monolayers. Biophys Chem 33: 63–70
Denicourt N, Tancrede P, Teissie J (1994) The main transition of dipalmitoylphosphatidylcholine monolayers: a liquid expanded to solid condensed high order transformation. Biophys Chem 49: 153–162
Discher BM, Maloney KM, Grainger DW, Sousa CA, Hall SB (1999) Neutral lipids induce critical behavior in interfacial monolayers of pulmonary surfactant. Biochemistry 38: 374–383
Du Noy PL (1919) A new apparatus for measuring surface tension. J Gen Physiol 1: 521–528
Egry I, Jacobs G, Schwartz E, Szekely J (1996) Surface tension measurements of metallic melts under microgravity. Int J Thermophys 17: 1181–1189
Evans RW (1995) Aggregates of saturated phospholipids at the air-water interface. Chem Phys Lipids 78: 163–175
Evans RW, Williams MA, Tinoco J (1980) Surface viscosities of phospholipids alone and with cholesterol in monolayers at the air-water interface. Lipids 15: 524–533
Fleming BD, Keough KM (1988) Surface respreading after collapse of monolayers containing major lipids of pulmonary surfactant. Chem Phys Lipids 49: 81–86
Franses EI, Basaran OA, Chang CH (1996) Techniques to measure dynamic surface tension. Curr Opin Colloid Interface Sci 1: 296–303
Hall SB, Bermel MS, Ko YT, Palmer HJ, Enhorning G, Notter RH (1993) Approximations in the measurement of surface tension on the oscillating bubble surfactometer. J Appl Physiol 75: 468–477
Herold R (1997) Aufbau und Einsatz eines Captive-Bubble-Surfactometers zur Untersuchung der Oberflächeneigenschaften pulmonalen Surfactants und anderer oberflächenaktiver Stoffe. PhD thesis, Humboldt-Universität zu Berlin
Keough KMW (1992) Physical chemistry of pulmonary surfactant in the terminal air spaces. In: Robertson B, Van Golde LMG, Battenburg JJ (eds) Pulmonary surfactant. Elsevier, Amsterdam, pp 109–164
Kraegel J, Kretzschmar G, Li JB, Loglio G, Miller R, Möhwald H (1996) Surface rheology of monolayers. Thin Solid Films 284/285: 361–364
Kretzschmar G, Li J, Miller R, Motschmann H, Möhwald H (1996) Characterization of phospholipid layers at liquid interfaces. 3. Relaxation of spreading phospholipid monolayers under harmonic area changes. Colloids Surf A 114: 277–285
Ladha S, Mackie AR, Harvey LJ, Clark DC, Lea EJ, Brullemans M, Duclohier H (1996) Lateral diffusion in planar lipid bilayers: a fluorescence recovery after photobleaching investigation of its modulation by lipid composition, cholesterol, or alamethicin content and divalent cations. Biophys J 71: 1364–1373
Lenard P (1887) Ueber die Schwingungen fallender Tropfen. Ann Phys Chem 30: 209–243
Li J, Miller R, Möhwald H (1996a) Phospholipid monolayers and their dynamic interfacial behaviour studied by axisymmetric drop shape analysis. Thin Solid Films 284/285: 357–360
Li JB, Miller R, Vollhardt D, Weidemann G, Möhwald H (1996b) Isotherms of phospholipid monolayers measured by a pendant drop technique. Colloid Polym Sci 274: 995–999
Lide DR (1998) Handbook of physics and chemistry. CRC Press, Boca Raton
Lin SY, Wang WJ, Lin LW, Chen LJ (1996) Systematic effects of bubble volume on the surface tension measured by pendant bubble profiles. Colloids Surf A 114: 31–39
MacDonald RC, MacDonald RI, Menco BP, Takeshita K, Subbarao NK, Hu LR (1991) Small-volume extrusion apparatus for preparation of large, unilamellar vesicles. Biochim Biophys Acta 1061: 297–303
Meban C (1981) Effect of lipids and other substances on the adsorption of dipalmitoylphosphatidylcholine. Pediatr Res 15: 1029–1031
Miller A, Möhwald H (1987) Diffusion limited growth of crystalline domains in phospholippid domains. J Chem Phys 86: 4258–4265
Mitchell DC, Straume M, Miller JL, Litman BJ (1990) Modulation of metarhodopsin formation by cholesterol-induced ordering of bilayer lipids. Biochemistry 29: 9143–9149
Möhwald H (1993) Surfactant layers at water surfaces. Rep Prog Phys 56: 653–685
Nag K, Keough KM (1993) Epifluorescence microscopic studies of monolayers containing mixtures of dioleoyl- and dipalmitoylphosphatidylcholines. Biophys J 65: 1019–1026
Nag K, Perez Gil J, Cruz A, Keough KM (1996a) Fluorescently labeled pulmonary surfactant protein C in spread phospholipid monolayers. Biophys J 71: 246–256
Nag K, Perez Gil J, Cruz A, Rich NH, Keough KM (1996b) Spontaneous formation of interfacial lipid-protein monolayers during adsorption from vesicles. Biophys J 71: 1356–1363
Putz G, Goerke J, Schurch S, Clements JA (1994) Evaluation of pressure-driven captive bubble surfactometer. J Appl Physiol 76: 1417–1424
Rayleigh FRS (1879) On the capillary phenomena of jets. Proc R Soc Lond 29: 71–97
Sauerland S, Lohöfer G, Egry I (1993) Surface tension measurements on levitated liquid metal drops. J Non-Cryst Solids 156–158: 833–836
Schurch S, Qanbar R, Bachofen H, Possmayer F (1995) The surface-associated surfactant reservoir in the alveolar lining. Biol Neonate 67: 61–76
Seitz HR, Heck M, Hofmann K-H, Alt T, Pellaud J, Seelig A (1999) Biochemistry 38: 7950–7960
Stewart JCM (1980) Colorimetric determination of phospholipids with ammonium ferrothiocyanate. Anal Biochem 104: 10–14
Taneva S, Keough KM (1994a) Pulmonary surfactant proteins SP-B and SP-C in spread monolayers at the air-water interface: I. Monolayers of pulmonary surfactant protein SP-B and phospholipids. Biophys J 66: 1137–1148
Taneva SG, Keough KM (1994b) Dynamic surface properties of pulmonary surfactant proteins SP-B and SP-C and their mixtures with dipalmitoylphosphatidylcholine. Biochemistry 33: 14660–14670
Tian Y, Holt RG, Apfel RE (1997) Investigation of liquid surface rheology of surfactant solutions by droplet shape oscillations – experiments. J Colloid Interface Sci 187: 1–10
Toelle A, Meier W, Greune G, Ruediger M, Hofmann K-P, Ruestow B (1999) Plasmalogens reduce the viscosity of a surfactant-like phospholipid monolayer. Chem Phys Lipids 10081–10087
Trinh E, Wang TG (1982) Large-amplitude free and driven drop-shape oscillations: experimental observations. J Fluid Mech 122: 315–388
Wang TG, Anilkumar AV, Lee CP (1996) Oscillations of liquid drops – results from usml-1 experiments in space. J Fluid Mech 308: 1–14
Worthman LAD, Nag K, Davis PJ, Keough KMW (1997) Cholesterol in condensed and fluid phosphatidylcholine monolayers studied by epifluorescence microscopy. Biophys J 72: 2569–2580
Yu SH, Possmayer F (1996) Effect of pulmonary surfactant protein A and neutral lipid on accretion and organization of dipalmitoylphosphatidylcholine in surface films. J Lipid Res 37: 1278–1288